

Investigation of ancient teeth using Raman spectroscopy and synchrotron radiation Fourier-transform infrared (SR- μ FTIR): mapping and novel method of dating

W. Al Sekhaneh^{a,e,*}, Y. H Akkam^b, G. Kamel^c, A. Drabee^d, J. Popp^e

^aFaculty of Archaeology and Anthropology, Yarmouk University-Irbid-Jordan

^bDepartment of medicinal chemistry and pharmacognosy, Faculty of Pharmacy, Yarmouk University-Irbid-Jordan

^cSynchrotron-light for Experimental Science and Applications in the Middle East, Alan - Jordan

^dJordan Atomic Energy Commission (JAEC), Shafa Bdran 11934, Amman, Jordan

^eLeibniz Institute of Photonic Technology, Albert-Einstein-Straße 9, 07745 Jena, Germany

Raman spectroscopy and Synchrotron Radiation Fourier-Transform Infrared (SR- μ FTIR): Mapping have been increasingly applied as a good tool in archaeological research. The chronology of ancient samples is an essential step in archeology, and carbon dating using atomic force microscopy is the main technique. Nevertheless, the availability of instrumentation, sample preparation, and cost are barriers that limit the wide usage. The study was aimed to develop a method utilizing Raman spectroscopy and Synchrotron Radiation Fourier-Transform Infrared (SR- μ FTIR) Mapping to identify ancient teeth and sort them chronologically. Furthermore, Raman spectroscopy was used to evaluate the preservation of collagen and the crystallinity of Apatite in ancient teeth. The age of fourteen ancient teeth descent from different individuals (8 from Roman period-1500BC and 4 from Byzantine period-641AD) was confirmed using carbon dating via atomic force spectrometry. The ancient teeth along with modern teeth were investigated using micro-Raman spectroscopy (oscillation and mapping). The typical Raman spectrum of the dentin for ancient samples was recorded and then compared to the modern teeth. The ratio of the phosphate PO_4^{3-} the band at 963 cm^{-1} to organic CH band at 2950 cm^{-1} was calculated for all samples. Raman mapping was recorded for cross-section teeth samples. The AMS data showed that the ages of the samples were 3400-3800 and 1240-1350 years for Roman and Byzantine teeth, respectively. The phosphate $\nu_1 PO_4^{3-}$ vibration band at (963 cm^{-1}) in ancient teeth was shifted 3 cm^{-1} toward higher wavenumber compared to modern dentin samples (960 cm^{-1}). The intensity and broadening of the carbonate apatite band at 1050 cm^{-1} were directly proportional to the aging. The intensity of the organic part triplet peaks at (2882, 2950, 2962) decreased with age. The ratio of phosphate band to organic C-H band was 0.346-0.388 and 0.122-0.136 for Roman and Byzantine teeth, respectively. According to the Raman mapping, the organic material in ancient teeth degraded and diffused, while in modern tooth it concentrated. Raman spectroscopy (intensity at 963 cm^{-1} to 2950 cm^{-1}) can be used as a qualitative tool to chronologically sort the archeological teeth samples before the use of carbon dating. The preliminary dating by Raman spectroscopy can recognize if a tooth or bone sample is archaeological or not. This step may save time and money and shall be assigned as a pre-request for AMS analysis. Raman mapping may help to explore archeological samples for best-preserved organic matter, hence identify the best candidates for further analysis (DNA extraction). In the future, the proposed method can be expanded and applied in specific cases in ancient osteology.

(Received February 25, 2021; Accepted June 8, 2021)

Keywords: Hydroxyapatite, Bone, Dentin, enamel, Amide, Teeth, Micro-Raman spectroscopy, AMS and dating, AMS

* Corresponding author: sekhaneh@yu.edu.jo

1. Introduction

Archaeometry—also known as archaeological science—is the application of scientific methods and techniques (physical, chemical, biological, earth sciences, and engineering) to the archeological investigation^(A). This field has been quickly expanding and adopting new methodologies (elemental composition, chromatography, carbon dating)^(A). Hence, the analysis of archeological objects requires knowledge in chemistry, physics, particularly degradation and decay processes.

In many cases, archeologists are forced to examine organic remains such as bone and teeth. Bones and teeth last much longer than the rest of a body, and they can reveal information about the health, age, and gender. However, the examined bone and teeth can be affected by several factors: intrinsic and extrinsic^(B). Intrinsic factors include the chemistry, size, shape, structure, and density of the sample, along with pathological changes. Extrinsic factors include groundwater, soil type, temperature, and air, along with the nature of local flora and fauna, method of burial, and human activity^(C). Therefore, the situation becomes more complicated than the reaction of the sample with previously applied preservatives or chemical materials.

Teeth and bones are mainly composed of Hydroxyapatite (HA), however, the teeth (96% wt) have a higher concentration than bones (70% wt). The HA in teeth varies from empirically derived HA, and HA found in bones, as the dental version, is often calcium deficient due to fluorine substitutions (Abou Neel, Aljabo et al. 2016). Even in the tooth, there is a variation in the distribution of HA. The carbonate HA content of dentine is 5%–6%, while in enamel it is 3%, and the HA crystal size in dentine is much smaller than those in enamel (Leventouri, Antonakos et al. 2009).

Age assignment probably is one of the crucial information for the archeologists, which can be obtained from the remaining teeth and bone. Radiocarbon dating was the first chronometric technique widely available to archeologists where it allowed researchers to directly date the organic remains often found in archaeological sites. Radiocarbon dating or age assignments can be carried using conventional decay (beta counting) or Direct ion counting using accelerator mass spectrometry (AMS) technique. However, AMS is more accurate and required fewer samples size (0.5–1 mg of carbon) than the conventional method of mass spectroscopy (0.5 to 10 g of carbon).

Probably the most important factor to consider when using radiocarbon dating in general - AMS in specific- is the external factors, where the surrounding environment can influence radiocarbon ages. The introduction of "artificial" carbon can influence the ages of dates making them appear older or younger than they are. Hence, rigorous pretreatment is needed to make sure contaminants have been eliminated and will not lead to substantial errors during the carbon dating process. However, the pretreatment in AMS is tedious and requires time and money. Even though the small sample size in AMS is an advantage, the control of contaminants will be difficult. Moreover, AMS -although a powerful tool- is also a costly one. Establishing and maintaining an AMS spectrometer costs millions of dollars.

Raman spectroscopy is a non-destructive and label-free technique in which laser light of a single wavelength is scattered from the surface of an object, collected, and analyzed. Raman spectroscopy represents an excellent method for characterizing the molecular nature of valuable archaeological samples and has been applied to artworks and artifacts, (Smith and Clark, 2004) fossilized charcoal, (Cohen-Ofri et al., 2006), pottery, stone, and glass (Ricciardi et al., 2009) from different ages. Moreover, Raman spectroscopy was applied to determine the structural and chemical analysis of mineralized hard tissue (bone and teeth) (Carden and Morris 2000) and to study the degradation of the organic part of such tissues(Edwards et al. 2001; Pestle et al. 2015).

This study is exploiting Raman spectroscopy for estimating the age of archeological teeth comparable to the AMS results. The ancient teeth were dated using excavated artifacts found at the archaeological site (pottery, glass, and metal objects). Furthermore, the teeth surface was investigated using Raman mapping. This study shows the integration of both spectroscopies specify and merit scattering experiments and apply it in the archaeometry.

2. Materials and experiments

- **Samples:** Two types of samples were investigated in this study: ancient and modern. Ancient teeth samples were provided by Prof. Zeidoun, Al-Muheisen. A total of 14 teeth were collected from an archaeological study from the sites *Al-Yasila and Tell-alHusn* in Jordan (Al-Muheisen-2012). The chronology of the samples is summarized in table 1. The modern teeth samples were provided by Dr.Nader Rawabdeh.

Table 1. Chronology of samples.

Site	Period	Date	No. of teeth	Dating method
<i>Al-Yasila and Tell-alHusn</i>	Middle Bronze Age	2000BC-1500BC	10	Pottery
<i>Al-Yasila and Tell-alHusn</i>	Byzantine	324AD-641AD	4	Pottery

- **Accelerator mass spectrometry (AMS):**
 - **Sample preparation:** The samples were treated with an ultrasonic bath in 18.2 MΩ DDH₂O to remove surface contaminants. After cleaning, the samples were dried and powdered to accelerate the procedure of collagen extraction for dating. Then samples were subjected to "AAA method" (Acid-Alkaline-Acid) treatment. Briefly, the powder was incubated in 1N HCl at 4 C, to eliminate possible traces of carbonates. then incubated with an alkaline humic acid with 0.5 N of NaOH at 15 C. Finally, the collagen was gelatinized by dissolving the residues in acidic water (pH=1) at 60 C for 16 hours. The collagen solutions were then filtered through prewashed 0.45 μm particle retention glass microfibre filters. The gelatinized collagen was separated from the insoluble residues of the matrix by centrifugation at 5000 rpm for 30 minutes. Then the gelatinized collagen was left to dry at 80°C.
 - **Method:** to eliminate the effect of CO₂ that may be generated as a by-product, the samples were subjected to combustion for 2 hours at 900 C in vacuum quartz tubes, sealed with copper oxide and silver wires. The oxide cupric provides the oxygen for the combustion and silver isolates the sulfur and halogens in solid forms. After the combustion, the CO₂ was purified cryogenically passing it through glasses of Ethanol/ice dry dewar to catch the water. The purified CO₂ was then collected in crystal glasses to transport them to the AMS (Tandem/ Erlangen) where ¹³C and ¹⁴C were measured.
- **Micro-Raman spectroscopy**
 - **Sample preparation:** The ancient teeth were pre-treated before measurement by immersion in sodium hypochlorite solution for 12 hours to remove adhering organic material from the tooth surfaces without affecting the internal structures. The samples were then directly measured without any further modification. For the mapping experiment, a cross-section of the tooth was obtained using a diamond saw.
 - **Method:** Two dimensional hyperspectral Raman images and spectra were collected using Raman spectrometer (RXN1 microprobe, Kaiser Optical System, USA), Laser light source as single-mode diode laser (model Xtra, Toptica, Germany) with 785 nm red wavelength emission, the intensity of 100 mW focused on the samples with 100 ×/ NA 0.9 objective (Nikon, Japan) was coupled to a microscope. The Raman signal was detected on a Peltier-cooled (-60°C), back-illuminated, deep-depletion CCD chip (Andor, Ireland). Spectra re-obtained over the spectral region of 308 to 3450 cm⁻¹ at a spectral resolution of 4 cm⁻¹.

Raman mapping was obtained using Raman spectrometer system (alpha300 R;WITec Instruments, Germany) excited by a frequency-doubled Nd:YAG laser at a wavelength 532 nm

focused onto the samples through an X20 Nikon objective with a single spectrum acquisition time of 0.5 seconds, the data were processed using image plus software and Origin Pro 18 (www.originlab.com).

- **Synchrotron Radiation Fourier-Transform Infrared (SR- μ FTIR)**

Synchrotron Fourier-Transform Infrared microspectroscopy data were collected at SESAME light source (Synchrotron light for Experimental Science and Applications in the Middle East, Jordan) utilizing the Infrared beamline. The endstation incorporates a Nicolet Continuum IR microscope (Thermo Fisher Scientific©, USA) equipped with liquid Nitrogen cooled MCT (Mercury Cadmium Telluride) detector and is coupled to the 8700 Thermo FTIR Spectrometer. Samples were mounted on Prior© scan motorized stage for data collection with Omnic© v. 9.2.41 software package (Thermo Fisher Scientific, USA). The endstation is purged with dry air to minimize the contribution of carbon dioxide, CO₂, and water vapor. Background spectra were collected to assess its spectral contribution. 128 co-added scans were recorded for the samples in reflection mode in the Mid-IR region 4000–650 cm⁻¹ at 6 cm⁻¹ spectral resolution, with Levels of Zero Filling 1, and Happ-Genzel apodization window. Infrared maps were acquired using the OMNIC Atlus™ v. 9.1.24 mapping software (Thermo Fisher Scientific©, USA), with a 15x Schwarzschild objective using a double path single masking aperture size of 20x20 μ m².

3. Results and discussion

Raman spectroscopy has been increasingly applied as a good tool in archaeological research (Tsuda, Ruben, and Arends 1996; Vandenabeele, Edwards, and Moens 2007). The spectroscopy is applied to identify the composite of the artifacts and to study the degradation of bone (Edwards et al. 2001; Pestle et al. 2015). Furthermore, Raman is a powerful technique to characterize the molecular structure of ancient materials. The scattered of light across a range of vibrational wavelengths makes it possible to detect the changes in apatite structure at the molecular level, which can be compared to semi-quantitative analysis using the relative concentrations of functional groups based on peak properties, height, shift, or peak area ratios or through substitution mechanism (Smith 1996; Surovell and Stiner 2001).

In general, Raman spectroscopy executed in most experiments is not an absolute quantitative method but mainly comparative. However, quantitative information can be obtained from single peaks with the relevant data treatment and careful consideration of the factors that affect the result (Smith and Dent 2019).

3.1. Raman

3.1.1. Ancient teeth Raman spectrum

At the onset, the typical Raman spectrum of the dentin was recorded, and peaks assignment was integrated into the spectrum (Figure-1). The organic part may be illustrated in the triplet at 2950 cm⁻¹, left 2882 and right 2982, and the peaks at 1681, 1670, 1637, 1452, 1426, and 1271 cm⁻¹. The inorganic (mineral) part sub-signals are characterized at the following wavenumbers 1030, 1050, 1073, 963, 593, and 430 cm⁻¹.

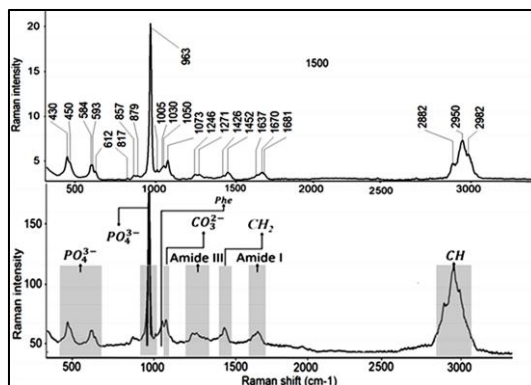


Fig. 1. Typical Raman spectrum of ancient dentin sample shows the main peaks of ancient dentin; these peaks contain chemical and structural information about ancient collagen and Apatite.

The organic part of teeth can be identified by the amide I and amide III peaks. Amide I located at (1637, 1670, and 1681 cm^{-1}) are mostly due to carbonyl stretching. Amide III band describes two vibrational modes at (1246 and 1271 cm^{-1}); stretching between carbon-nitrogen atoms and bending of a secondary amine, the bonds are of interest for teeth compositional studies (??). Bending of methylene groups ν [CH_2] and stretching between carbon and hydrogen atoms ν [$\text{C}-\text{H}$] are vibrational modes common to several peptides at 1426, 1452, 2882, 2950, 2982 cm^{-1} . Raman signal positioned at 1005 cm^{-1} is attributed to the aromatic breathing mode, it is specific to C- H in-plane bending mode with a stretching vibration of the phenylalanine ring (ν [Phe]) (Morris, Mandair et al. 2011).

The inorganic part of the teeth is attributed to apatite (phosphate and carbonate) signals. The most intense, sharp band at 963 cm^{-1} is attributed to the symmetrical stretching mode of ancient phosphate (ν_1 [PO_4^{3-}]) (figure-2). Several smaller bands were characterized as stretching and bending modes of phosphate groups at 450, 584, and 1030, 1050 cm^{-1} . The bands at 1050 and 1073 cm^{-1} may be assigned to carbonate groups.

3.1.2. Modern vs ancient teeth

The Raman study of the teeth reveals several differences between modern and ancient teeth spectrum at the following wavenumber; 960, 1050, and triplet (2882, 2950, 2962) cm^{-1} .

In all Raman dentin spectra, the ancient phosphate ν_1 PO_4^{3-} vibration band at (963 cm^{-1}) is shifted 3 cm^{-1} toward higher wavenumber compared to modern dentin samples (960 cm^{-1}) (figure 2). This effect may be explained by the substitution of fluoride for OH in teeth generating fluoroapatite. The band shifting gives information about the structure and crystallinity of Apatite, which may be related to the age of the tooth. This phenomenon may be useful to determine qualitatively the age of the teeth, however, due to the lack of different age samples, it can't determine the age of each tooth.

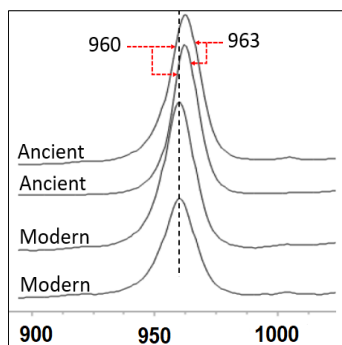


Fig. 2. The ancient ν_1 PO_4^{3-} vibration band of ancient dentin sample from Tell al-Husn at (963 cm^{-1}) shifted 3 cm^{-1} toward higher wave number compared to modern dentin samples at (960 cm^{-1}).

The band at 1050 cm^{-1} was assigned to the carbonate apatite, where the intensity and broadening are directly proportional to the time, as illustrated in Fig. 3. The organic part of teeth degrades more rapidly than the mineral part during the burial conditions and chemical alterations.

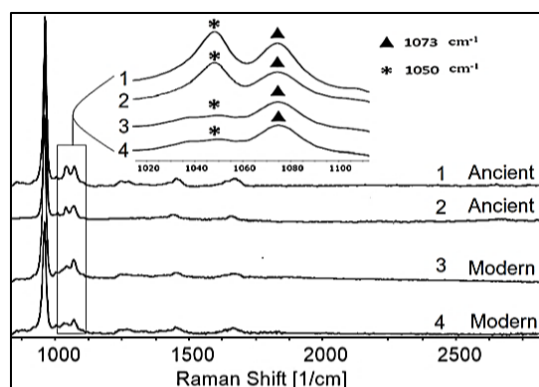


Fig. 3. The hydroxyapatite peaks of dentin at 1050 cm^{-1} and carbonate at 1073 cm^{-1} of modern and ancient dentin, the peaks began to appear clearly separate in ancient teeth.

In general, the organic part (collagen) controls the dynamic system of the degradation process of the matrix (organic and inorganic). Moreover, the degradation of the organic part of collagen alters the orientation of carbonate crystals. Therefore, this phenomenon may be explained by B-type substitution. There are two types of carbonate substitutions are present in teeth: A-type (carbonate for phosphate) and B-type (carbonate for hydroxyl). However, most diffused is B-type *. Furthermore, the broadening of the signal may be related to carbonate crystallinity. Previously it has been reported that, with age, the crystallinity of dental HA decreased but the carbonate content increased (*).

Another variation between ancient and modern teeth appeared at the triplet peaks at (2882, 2950, 2962) (Fig. 4). Moreover, this peak completely disappeared in enamel compare to dentin. This peak was assigned as the C-H organic peak. The concentration of organic matter is varied between dentine (> 20%) and enamel (<1.5%) (Pajor, Pajchel et al. 2019). The very low concentration of organic matter explains the absence of the triplicate peak in enamel analysis. It is already known that the organic part is degraded with time, therefore it makes sense that the intensity of the peak decreased in the ancient teeth compared to the modern tooth (Fig. 4).

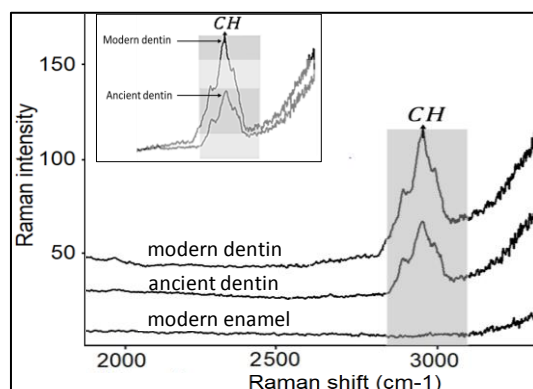


Fig. 4. Raman spectrum shows the triplet peak of organic part (C-H) of modern dentin; ancient dentin; and modern enamel. The upper graph shows the overlap between the modern and ancient dentin.

The main interest lies in the spectral domain corresponding to the functional groups of the inorganic region of the phosphate groups, as well as, the carbonate and proteins organic region (from 800 cm^{-1} to 3000 cm^{-1}). In general, for both the ancient and the modern samples, the processed spectra demonstrated distinguishing spectral features of the teeth matrix [1, 2, 3]. In

particular, (1) the phosphate region, with a very intense maximum included in the interior of a sequence of low-intensity sub-bands and shoulders signifying the inorganic (mineral matrix) were observed successively within the spectral region of 800-1100 cm^{-1} those are commonly attributed to the presence of a number of phosphate derivatives, (2) consecutive peaks in the range 1400 - 1500 cm^{-1} those are associated to the occurrence of carbonate bands, and (3) the organic groups situated within the region 2800-3000 cm^{-1} , (4) the main protein contribution that is recognized in the region of 1500-1700 cm^{-1} . Additional organic signatures were also noted within the 2800-3000 cm^{-1} region. Peak assignment details are given in Table 2.

Table 2. Peak assignment of the modern and the ancient teeth cross-sections. (Seredin, et al., 2020).

Functional groups	Vib. mode	IR assignment, cm^{-1}	Modern teeth P4	Ancient teeth 725
$\nu_1\text{CO}_3$ A-type	C-O	870	870	866
$\nu_1\text{PO}_4$	P-O str.	956.6	960	955
$\nu_3\text{PO}_4$	P-O antysym. Str.	1040, 1048, 1060, 1090	1038, 1087	1034, 1061, 1094
$\nu_1\text{CO}_3$ B-type $\nu_1\text{CO}_3$ AB-type/ CH_3	C-O	1401.3, 1445	1403, 1445	1409, 1439
$\nu_1\text{CO}_3$ A-type Amide II	C-O	1540	1541	1543
Amide I	C-O and C-N str.	1600-1700	1602, 1629, 1649, 1683	1614, 1633, 1657, 1682

3.1.3. Proposed ratio

Since both peaks CH Raman at 2950 cm^{-1} and the phosphate PO_4^{3-} at 963 cm^{-1} are specific to the ancient tooth and their intensity is time-dependent, both peaks might be utilized qualitatively to assign the tooth age. The ratio was calculated according to the following equation: $\frac{\text{intensity at } 963 \text{ cm}^{-1}}{\text{intensity at } 2950 \text{ cm}^{-1}}$. Table 3 summarizes the ratio of all tested samples.

Table 3. The proposed ratio of tested samples. intensity of 963 cm^{-1} /2950 cm^{-1} using Raman spectroscopy.

Sample No.	1	2	3	4	5	6	7	8	9	10	11	12	13	14
Ratio 963/2950	0.13 0	0.12 9	0.12 4	0.13 5	0.34 8	0.38 8	0.35 5	0.38 5	0.38 8	0.35 2	0.35 3	0.38 0	0.34 6	0.35 0

3.2. Age determination and carbon dating:

The consultation of scientific methods of materials classification, in combination with archaeology by typological classification of the archaeological material, will ultimately enable us to be more specific in materials exploration. Hence, the chronology of tested samples was determined using the typological classification (pottery) and then confirmed using carbon dating via AMS. Tested teeth samples were dated to the Roman and Byzantine period, around 1550BC and 640 AD, respectively (Al-Muheisen-2012). Figure 5 shows an example of the AMS data. Radiocarbon dating of the dentine yielded a conventional C^{14} age of 1289 ± 53 yr BP. Following calibration using the IntCal13 atmospheric curve Ramsey and Lee 2013; Reimer et al. 2013. The raw data are represented by the standard green curve of distribution on the horizontal axis, now, to be calibrated with the help of the calibration curve-the wiggly red dashed line-in order to gain calendar years. The straightforward interception method at one or two standard deviations visually

examines the overlap between the measurement made and the reference curve. In contrast, the standard method is used to calculate a probability density function for the age of the sample with the help of a calibration program.

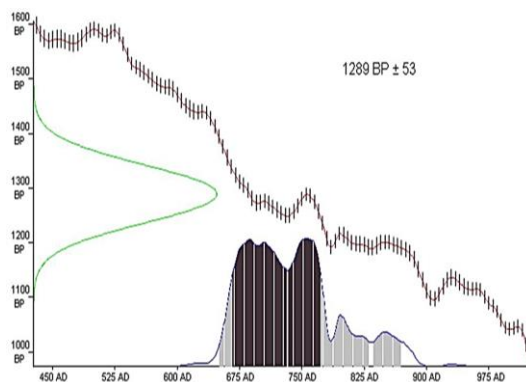


Fig. 5. Radioarbon C14 Dating of an ancient tooth. The calibration of radiocarbon age 1289 ± 53 yr BP (left in green), dentine at the 95.4% confidence level. The calibrated date is 650 to 870 cal yr CE

3.3. Correlation of the proposed ratio with carbon dating data

As illustrated in figure 6, the AMS result split into two categories according to age; 1100-1300 and 3100-3700 years as well as the ratio between 963/2950 divided in the same manner. There is a proportional relationship between the age and the ratio of 963/2950, as the age increases the ratio increase. The relative intensities of the organic part to phosphate part increases with the degradation of the organic part which is directly proportional to the age of the sample. To some extent, the ratio of 963/2950 can give an estimate of the age of the sample. Therefore, Raman analysis might be used for Relative dating.

The ^{14}C -dating is much more expensive than Raman spectroscopy, therefore the samples can be separated initially according to their relative age by Raman measurements, and afterward, the oldest samples will be sent for the analysis using ^{14}C .

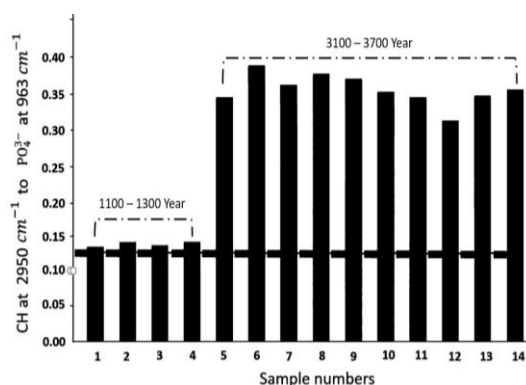


Fig. 6. Age assignment using Raman Data. The ratio of intensity at 2950 to the intensity at 963, and assigned age using carbon dating data (AMS).

3.4. Raman mapping

Teeth and bones are frequently the only sources of DNA available for identification of degraded or fragmented human remains. The unique composition of teeth and their location in the jaw bone provide additional protection to DNA compared to bones making them a preferred source of DNA in many cases. Enamel acts as a protection to dentin and underlying nerve and at least under the enamel and dentin, it is possible to get DNA as covered in Dental DNA fingerprinting in the

identification of human remains. Moreover, the possible contamination of bone is high compare to teeth as the pore size in bone is much larger than on the teeth surface.

Raman spectroscopy can provide valuable information related to collagen preservation; therefore, Raman mapping can be utilized to determine the quality of collagen before measuring the DNA (Khalid, Bora et al. 2018). The results are shown as a three-dimensional cube where two dimensions depict the spatial distribution of the chemical compounds while the third one, the spectral dimension, allows the identification of the chemical compounds to determine the macroscopic distribution of these compounds.

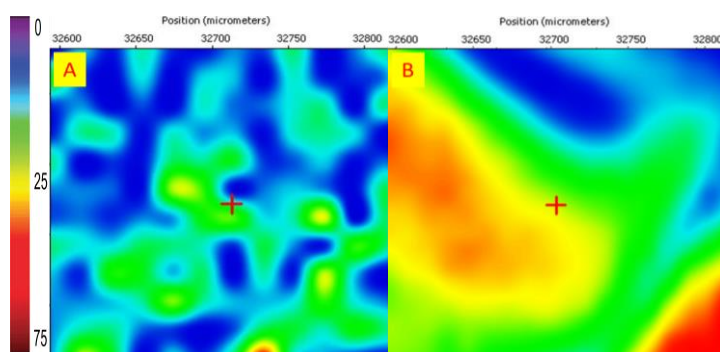


Fig. 8. Raman mapping showing the distribution of organic matters in the dentin of A) ancient and B) modern tooth.

As illustrated in Fig. 8, the variation in the distribution of organic material is clear between ancient and modern teeth. In ancient tooth (A-Fig. 8), the organic material is degraded and diffused, while in modern tooth it is concentrated (B-Fig. 8). Hence, the quality of organic material in the ancient sample (B) is not a good candidate for DNA extraction. Such info may save time and money for researchers and help to explore the samples to select the best candidates.

3.5. SR- μ FTIR chemical mapping

As shown in Fig. 9, the chemical distribution of cross section teeth was investigated using different vibrational modes. The maps were created for the inorganic region ($900\text{--}1100\text{ cm}^{-1}$), the protein Amide I, and for the organic contributions of the high wavenumber region ($2800\text{--}3000\text{ cm}^{-1}$) as well. Also, the carbonate region chemical maps are depicted for both teeth. The SR- μ FTIR emphasized the degradation of the organic part which is represented by Amide and organic bands. Moreover, the carbonate signal represents the substitution process in ancient teeth structures.

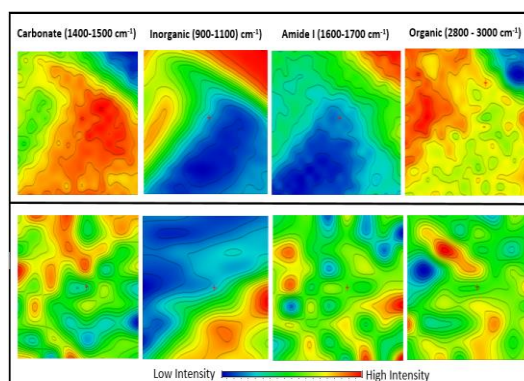


Fig. 9. Chemical IR maps generated from the overall cross-section of (first row) the modern reference, (second row) ancient tooth depicting the integrated intensity of the Amide I absorption band, as well as, the inorganic and the carbonate regions.

4. Conclusions

Raman spectroscopy and SR- μ FTIR have an excellent measuring efficiency for organic and mineral parts of teeth. Raman spectroscopy is an easy, available, cheap method to classify the samples whether they are modern or ancient. Firstly, the proposed ratio ($963\text{ cm}^{-1}/2950\text{ cm}^{-1}$) may serve as an indicator for aging as it correlates proportionally with aging and is suited well with the C14 dating. Secondly, the phosphate ν_1 vibration in the ancient dentin was shifted toward a high wavenumber (963 cm^{-1}). Thirdly, the intensity of hydroxyapatite peak at 1050 cm^{-1} in ancient dentin, which is related to the carbonate substitution due to the long burial duration.

Raman spectroscopy can be used as a qualitative tool to chronologically sort the archeological teeth samples before the use of carbon dating. This tool may save time and money and shall be assigned as a pre-request for AMS analysis, especially for large samples. Raman mapping may help to explore archeological samples (teeth and bone) for the highest purity and quality of organic matter, hence identify the best candidates for DNA extraction. In the future, the proposed method can be expanded and applied in specific cases in ancient osteology.

Acknowledgments

The researchers are grateful to the German Research Society (DFG) for financial support and IPHT Jena Germany, particularly grateful to Prof. Jürgen Popp the Director of Leibniz IPHT and the Chair of Physical chemistry at Friedrich-Schiller-University Jena and Prof. Wolfgang Kretschmer, Dr. Andreas Scharf, and K. Kritzler in AMS beamline at the Erlangen tandem accelerator. Special thanks to Prof. Dr. Khaled Toukan / director of Jordan Atomic Energy Commission (JAEC) and SESAME project.

References

- [1] E. A. Abou Neel, A. Aljabo, A. Strange, S. Ibrahim, M. Coathup, A. M. Young, L. Bozec, V. Mudera, *International journal of nanomedicine* **11**, 4743 (2016).
- [2] Z. Al-Muheisen, *Newsletter of Faculty of Archaeology and Anthropology* **88**, 1 (2009).
- [3] Z. Al-Muheisen, *Palestine exploration quarterly* **144**(2), 84 (2012).
- [4] G. Anneroth, K.-A. Norberg, *Acta Odontol. Scand.* **26**(1-2), 89 (1968).
- [5] M. Anwar Alebrahim, C. Krafft, W. Sekhaneh, B. Sigusch, J. Popp, *Biomedical Spectroscopy and Imaging* **3**(1), 15 (2014).
- [6] M. Bath-Balogh, M. J. Fehrenbach, *Illustrated Dental Embryology, Histology, and Anatomy - E-Book*, Elsevier Health Sciences, 2014.
- [7] M. M. Beasley, E. J. Bartelink, L. Taylor, R. M. Miller, *Journal of Archaeological Science* **46**, 16 (2014).
- [8] L. H. Berman, K. M. Hargreaves, S. R. Cohen, *Cohen's Pathways of the Pulp Expert Consult - E-Book*: Elsevier Health Sciences, 2010.
- [9] F. Bodart, G. Deconninck, M. T. Martin, *IEEE Transactions on Nuclear Science* **28**(2), 1401 (1981).
- [10] G. Bonel, *Contribution à l'étude de la carbonatation des apatites, presentee a l'Universite Paul Sabatier de Toulouse pour obtenir le grade de ...*, 1970.
- [11] A. L. Boskey, *Current osteoporosis reports* **4**(2), 71 (2006).
- [12] A. Carden, M. D. Morris, *Journal of biomedical optics* **5**(3), 259 (2000).
- [13] A. Casasco, A. Calligaro, M. Casasco, D. Springall, J. Polak, P. Poggi, C. Marchetti, *Histochemistry* **95**(2), 115 (1990).
- [14] B. Cengiz, Y. Gokce, N. Yildiz, Z. Aktas, A. Calimli, *Colloids and Surfaces A: Physicochemical and Engineering Aspects* **322**(1-3), 29 (2008).
- [15] C. Chadefaux, A.-S. Le Hô, L. Bellot-Gurlet, I. Reiche, *2e-Preservation Science* **6**, 129 (2009).
- [16] H. Edwards, D. Farwell, D. De Faria, A. Monteiro, M.C. Afonso, P. De Blasis, S. Eggers,

- J. Raman Spectrosc. **32**(1), 17 (2001).
- [17] J. Elliott, Paper read at J. Dent. Res., 1963.
- [18] M. H. Fathi, A. Hanifi, *Materials Letters* **61**(18), 3978 (2007).
- [19] C. A. France, D. B. Thomas, C. R. Doney, O. Madden, *Journal of Archaeological Science* **42**, 346 (2014).
- [20] N. Garg, A. Garg, *Textbook of Operative Dentistry: Jaypee Brothers, Medical Publishers Pvt. Limited*, 2010.
- [21] I. R. Gibson, W. Bonfield, *Journal of Biomedical Materials Research: An Official Journal of The Society for Biomaterials, The Japanese Society for Biomaterials, and The Australian Society for Biomaterials and the Korean Society for Biomaterials* **59**(4), 697 (2002).
- [22] M. M. Houck, *Forensic Anthropology: Elsevier Science*, 2016.
- [23] A. Ito, K. Maekawa, S. Tsutsumi, F. Ikazaki, T. Tateishi, *Journal of Biomedical Materials Research: An Official Journal of The Society for Biomaterials and The Japanese Society for Biomaterials* **36**(4), 522 (1997).
- [24] M. Khalid, T. Bora, A. Al Ghaithi, S. Thukral, J. Dutta, *Scientific reports* **8**(1), 1 (2018).
- [25] G. C. Koumoulidis, A. P. Katsoulidis, A. K. Ladavos, P. J. Pomonis, C. C. Trapalis, A. T. Sdoukos, T. C. Vaimakis, *J. Colloid Interface Sci.* **259**(2), 254 (2003).
- [26] M. Lebon, I. Reiche, F. Fröhlich, J.-J. Bahain, C. Falguères, *Analytical and bioanalytical chemistry* **392**(7-8), 1479 (2008).
- [27] R. Le Geros, O. Trautz, J. Le Geros, E. Klein, Paper read at Bull. Soc. Chim. Fr., 1968.
- [28] T. Leventouri, A. Antonakos, A. Kyriacou, R. Venturelli, E. Liarokapis, V. Perdikatsis, *International Journal of Biomaterials* **2009**, Article ID 698547 (2009).
- [29] H. S. Liu, T. S. Chin, L. S. Lai, S. Y. Chiu, K. H. Chung, C. S. Chang, M. T. Lui, *Ceramics International* **23**(1), 19 (1997).
- [30] N. Lynnerup, H. D. Klaus, In *Ortner's Identification of Pathological Conditions in Human Skeletal Remains: Elsevier*, 2019.
- [31] D. T. Millett, R. Welbury, *Orthodontics and Paediatric Dentistry: Churchill Livingstone*, 2000.
- [32] M. D. Morris, G. S. Mandair, *Clinical Orthopaedics and Related Research®* **469**(8):, 2160 (2011).
- [33] R. Murugan, S. Ramakrishna, *Composites Science and Technology* **65**(15-16), 2385 (2005).
- [34] G. Nagy, T. Lorand, Z. Patonai, G. Montsko, I. Bajnoczky, A. Marcsik, L. Mark, *Forensic science international* **175**(1), 55 (2008).
- [35] F. Nakano, H. Takahashi, F. Nishimura, *Dent. Mater. J.* **18**(3), 304 (1999).
- [36] E. A. A. Neel, A. Aljabo, A. Strange, S. Ibrahim, M. Coathup, A. M. Young, L. Bozec, V. Mudera, *International journal of nanomedicine* **11**, 4743 (2016).
- [37] D. Nelson, J. Featherstone, *Calcif. Tissue Int.* **34**, S69 (1982).
- [38] H. Oonishi, *Biomaterials* **12**(2), 171 (1991).
- [39] K. Pajor, L. Pajchel, J. Kolmas, *Materials* **12**(17), 2683 (2019).
- [40] L. C. Palmer, C. J. Newcomb, S. R. Kaltz, E. D. Spoerke, S. I. Stupp, *Chem. Rev.* **108**(11), 4754 (2008).
- [41] P. Parhi, A. Ramanan, A. R. Ray, *Materials Letters* **58**(27-28), 3610 (2004).
- [42] S. H. Park, L. Ye, R. M. Love, J.-C. Farges, H. Yumoto, *Mediators Inflamm.*, 2015.
- [43] E. Paschalis, E. DiCarlo, F. Betts, P. Sherman, R. Mendelsohn, A. Boskey, *Calcif. Tissue Int.* **59**(6), 480 (1996).
- [44] W. J. Pestle, V. Brennan, R. L. Sierra, E. K. Smith, B. J. Vesper, G.A. Cordell, M. D. Colvard, *Journal of Archaeological Science* **58**, 113 (2015).
- [45] L. Pramatarova, *On Biomimetics: IntechOpen*, 2011.
- [46] H. R. Ramay, M. Zhang, *Biomaterials* **24**(19), 3293 (2003).
- [47] C. B. Ramsey, S. Lee, *Radiocarbon* **55**(2), 720 (2013).
- [48] I. Reiche, L. Favre-Quattropiani, C. Vignaud, H. Bocherens, L. Charlet, M. Menu, *Measurement Science and Technology* **14**(9), 1608 (2003).
- [49] I. Reiche, C. Vignaud, M. Menu, *Archaeometry* **44**(3), 447 (2002).
- [50] P. J. Reimer, E. Bard, A. Bayliss, J. W. Beck, P. G. Blackwell, C. B. Ramsey, C. E. Buck, H. Cheng, R. L. Edwards, M. Friedrich, *Radiocarbon* **55**(4), 1869 (2013).

- [51] C. Rey, B. Collins, T. Goehl, I. Dickson, M. Glimcher, *Calcif. Tissue Int.* **45**(3), 157 (1989).
- [52] V. M. Rusu, C.-H. Ng, M. Wilke, B. Tiersch, P. Fratzl, M. G. Peter, *Biomaterials* **26**(26), 5414 (2005).
- [53] A. J. Salgado, O. P. Coutinho, R. L. Reis, *Macromol. Biosci.* **4**(8), 743 (2004).
- [54] P. Seredin, D. Goloshchapov, Y. Ippolitov, J. Vongsvivut, *Scientific Reports* **10**(1), 1 (2020).
- [55] B. C. Smith, *Fundamentals of Fourier Transform Infrared Spectroscopy*, CRC Press, Boca Raton, 1996.
- [56] E. Smith, G. Dent, *Modern Raman Spectroscopy: A Practical Approach*: Wiley, 2019.
- [57] E. T. Stathopoulou, V. Psycharis, G. D. Chryssikos, V. Gionis, G. Theodorou, *Palaeogeography, Palaeoclimatology, Palaeoecology* **266**(3–4), 168 (2008).
- [58] W. Suchanek, M. Yashima, M. Kakihana, M. Yoshimura, *Biomaterials* **18**(13), 923 (1997).
- [59] T. A. Surovell, M. C. Stiner, *Journal of Archaeological Science* **28**(6), 633 (2001).
- [60] L. Tanchev, *Virtual and Rapid Manufacturing: Advanced Research in Virtual and Rapid Prototyping*: CRC Press, 2007.
- [61] T. J. U. Thompson, M. Islam, M. Bonniere, *Journal of Archaeological Science*, 2012.
- [62] H. Tsuda, J. Ruben, J. Arends, *Eur. J. Oral Sci.* **104**(2), 123 (1996).
- [63] P. Vandenabeele, H. G. Edwards, L. Moens, *Chem. Rev.* **107**(3), 675 (2007).
- [64] M. Vignoles, G. Bonel, R. Young, *Calcif. Tissue Int.* **40**(2), 64 (1987).
- [65] R. Wallaey, *Colloquium of the International Union of Pure and Applied Chemistry, Munster, Verlag Chemie: Weinheim, Germany, 1954.*
- [66] M. Walters, Y. Leung, N. Blumenthal, K. Konsker, R. LeGeros, *J. Inorg. Biochem.* **39**(3), 193 (1990).
- [57] S. Weiner, P. Goldberg, O. Bar-Yosef, *Journal of Archaeological Science* **20**(6), 613 (1993).